Investigation on low-speed pre-ignition from the quantification and identification of engine oil droplets release under ambient pressure conditions

Bernardo Tormos[a], José María García[a], Sophia Bastidas[a,*], Beatriz Domínguez[b], Fermin Oliva[b], Dolores Cárdenas[b]

[a] *CMT-Motores Térmicos, Universitat Politècnica de València. Camino de Vera S/N, 46022. Valencia, Spain.*
[b] *REPSOL. C/ Agustín de Betancourt S/N, 28935. Móstoles, Spain.*

Abstract

One source of low-speed pre-ignition in turbocharged gasoline direct injection engines is the presence of oil droplets in the combustion chamber. In this study, oil droplets released due to the piston reciprocating motion, have been quantified as function of oil viscosity and engine speed, by means of a motored test rig under ambient pressure conditions. Oil droplets were collected using a sandwich-like support and absorbing paper. An image processing methodology was developed to identify critical regions of the piston prone to the appearance of oil. Results show that oil is scrapped by the piston rings and released to the combustion chamber in zones transverse to the piston pin, at speeds as low as 500 rpm. Oil viscosity does not have a determining effect on the oil amount reaching the combustion chamber, while engine speed greatly increases this phenomenon, with a critical point at 2500 rpm and oil temperature of 80°C.

Keywords: Engine oil, Oil droplets, Low-speed pre-ignition, Image processing

*Corresponding author
Email address: kabasmon@mot.upv.es (Sophia Bastidas)

April 19, 2020

1. Introduction

Low-speed pre-ignition (LSPI) is a phenomenon occurring in downzised boosted gasoline direct injection (GDI) engines, where uncontrolled, abnormal combustion events take place as a consequence of high in-cylinder pressures found in modern engines [1, 2]. This combustion, occurring too early in the stroke, can cause serious damage to the piston-cylinder assembly, as the piston has not yet reached the top dead center (TDC) [3, 4, 5].

With fuel economy standards pushing forward to further reduce emissions, downsizing and turbocharging will continue to be adopted in new gaoline powered vehicles [6, 7], and therefore to be operated at regimes (low engine speed) and loads (high load) where LSPI events are more likely to occur. This phenomenon is therefore a setback to continue the development of these technologies and new engine designs, affecting fuel economy improvements and the reduction of emissions [8, 9].

LSPI events have been found to be caused by the interaction of different parameters, such as fuel, lubricating oil, engine design and its operation [10, 4, 11, 8, 12, 13, 14]; therefore, to reduce the occurrence of this phenomenon, all the contributing factors need to be understood and tackled. One of the principal hypothesis for the occurrence of LSPI involves the interaction of fuel and engine oil [4, 15, 16, 17]. On one hand, liquid fuel films formed in the liner interact with the oil forming a mixture of which, two characteristics are determining for the auto-ignition, oxidation and evaporation [8]. On the other hand, this interaction results in changes of the oil properties, such as viscosity and surface tension, making it more prone to the release of droplets to the combustion chamber. The droplets may have a reduced ignition delay time, as a consequence of the higher reactivity of the larger size molecules of lubricating oil.

In this way, studies are still needed regarding the oil released to the combustion chamber, its phase (liquid or gas), quantity and chemical composition, that allow to determine the reactivity of the mixture, and therefore its tendency to ignite [15]. In the work developed by Ito et al [18], for instance, some tests were developed on how oil droplets reach the combustion chamber using high speed cameras. Three sources of oil droplets were analyzed, piston crevice, piston crown and ring gap. They found that oil droplets from ring crevice are released in every stroke, while droplets from the piston crown are arbitrary. Some studies have found that formulations with a low reactivity base and low propensity to absorb fuel, can help to reduce LSPI [19, 15].

A comprehensive study of the oil parameters and working conditions that promote the oil droplets release is another approach yet to be fully understood. Dahnz et al [3] for instance, found that oil dilution greatly affects the amount of oil droplets released, which in turn is affected by the position of the injector.

Recent studies have been developed on the chemical composition of the oil leading to LSPI events, and one of the main conclusions has been the negative effect of the Ca-based additive [20, 21, 22, 23, 24, 25]. In response to the different findings on the effect of the engine oil on LSPI, the American Petroleum Institute (API) launched, at the end of 2017, a new classification, denoted as SN PLUS, for oils including an additional protection against LSPI for turbocharged GDI engines [26, 27]. The new standard proposed by the International Lubricants Standardization and Approval Committee (ILSAC), denoted as ILSAC GF-6, will also include a test for LSPI events related to the oil formulation [28].

With the LSPI as a barrier for future developments of internal combustion engines for fuel economy and greenhouse gas emissions reduction, it is of great importance to fully identify and understand the factors that promote the appearance of this phenomenon. The study presented here aims at presenting a simple methodology to quantify the oil droplets release, and an image processing methodology to identify critical regions of the combustion chamber prone to the appearance of oil. Results are presented on the effect of the oil viscosity and engine speed over the quantity of oil droplets and its distribution in the combustion chamber.

2. Materials and Methodology

2.1. Experimental setup

The test rig used in this study is a modification of a previously designed test rig for friction force measurements, known as floating liner. It consists of a single-cylinder, four-stroke internal combustion engine with modifications to isolate the cylinder liner from the engine structure, and force sensors to capture the friction force. The cylinder head and upper part of the engine block were removed and replaced by the structure of the floating liner. For the study presented here, further modifications were developed in the rig. The piston was replaced for a gasoline-type reference with a bore diameter of 93 mm, and the liner was changed to meet the piston dimensions. The

Bore	mm	93
Stroke	mm	90
Piston length	mm	84.95
Piston - liner clearance	mm	0.02
Lubrication system	-	wet sump

Table 1: Main characteristics of the test engine

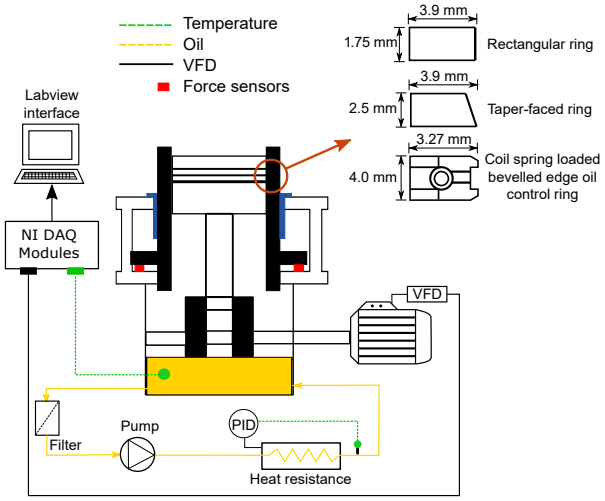

Figure 1: Schematic diagram of the experimental setup

main characteristics of the test engine are summarized in Table 1. The floating liner structure was modified to allow an easy access to the combustion chamber, and therefore to be able to measure the oil droplets scattered to the chamber. The test rig worked without combustion and under ambient pressure conditions, motored by means of an electric motor with a variable frequency drive (VFD) to set the engine speed for the tests. The rig comprises a lubrication system with a heat resistance, thermocouples and a PID (proportional-integral-derivative) controller to set the oil temperature. The operation and data acquisition (DAQ) of the test rig was implemented in modules of National Instruments and a Labview interface. Figure 1 is a schematic diagram of the experimental setup, including some specifications of the piston rings employed in the study.

To collect the oil droplets scattered to the combustion chamber, the absorbing paper was held with a sandwich-like support shown in Figure 2. It

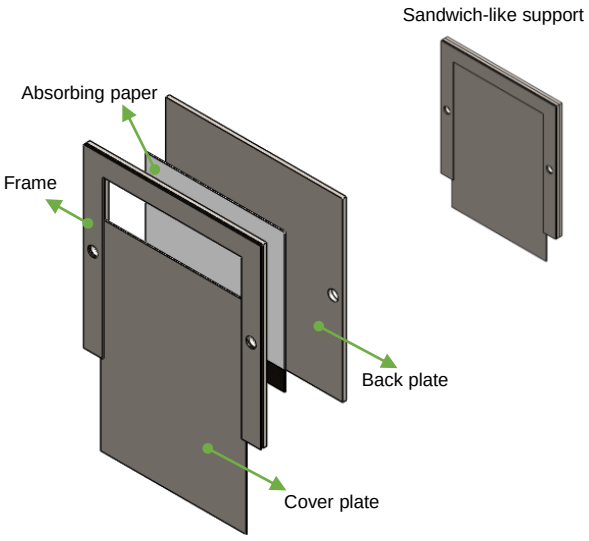

Figure 2: Support structure for the absorbing paper

consists of a back plate, a cover plate to protect the absorbing paper, and a frame that allows to remove the cover plate, leaving the paper exposed to the oil droplets during test. This support was located over the cylinder liner at a predefined distance from the top rim. Figure 3 a) shows the test rig used for the tests; and Figure 3 b) and d) show the isometric an top view of the setup of the absorbing paper. As it can be seen from the top view, the absorbing paper was located upside down to absorb the oil; then, to weigh the oil mass and for image processing, the paper was turned as shown in Figure 3 c). The black square in the lower right corner of the paper was used to write the reference number for each test.

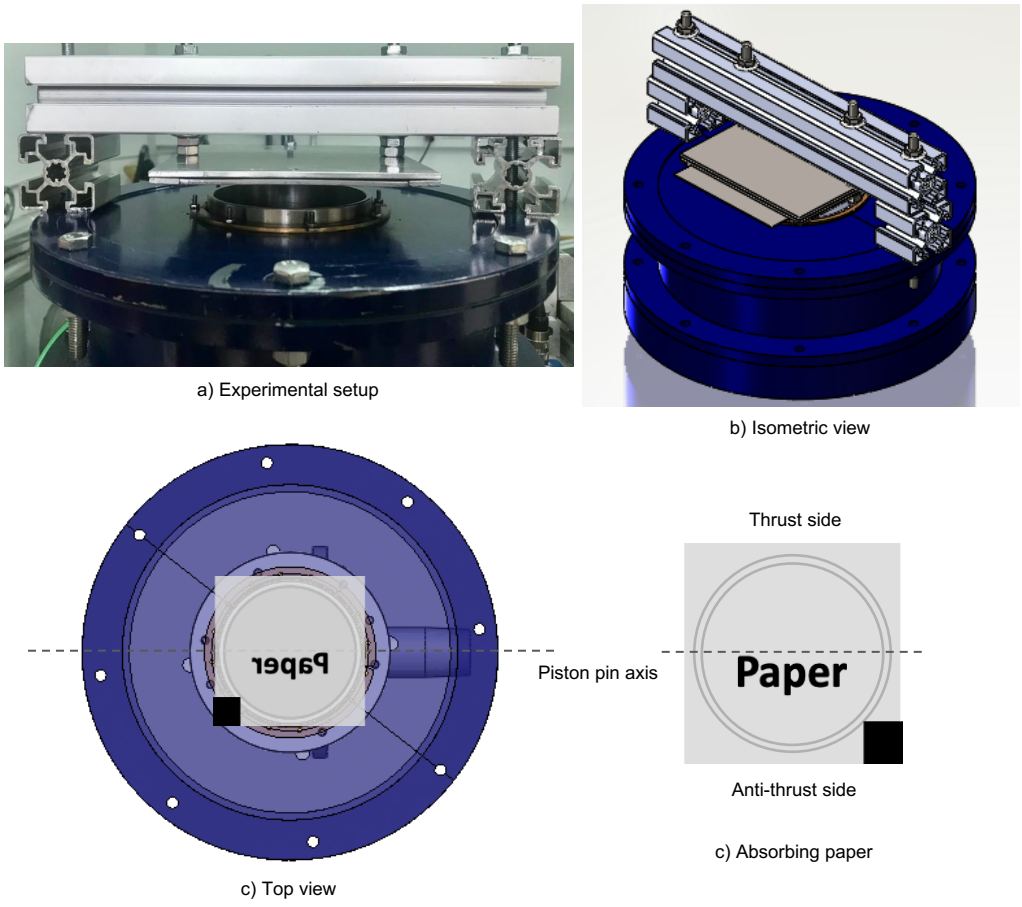

Figure 3: Setup of the absorbing paper in the test rig. a) Experimental set up. b) Isometric view of the upper part of the test rig. c) Top view of the rig. d) Paper used for oil mass weighing and image processing

2.2. Oil formulation

As it was mentioned in the introduction, oil viscosity and engine speed are the two parameters aimed to be evaluated in this study. For the former, in order to have different levels of viscosity values, two possible test configurations were discussed. First, using oil formulations of different SAE (Society of Automotive Engineers) grade; and second, using one oil formulation varying its working temperature.

Measurements of kinematic viscosity and density were developed for five engine oil formulations of different SAE grade, 5W30, 0W20, 0W16, 0W12 and 0W8, at a range of temperatures, from 40 to 100°C. The kinematic vis-

cometer SVM 3001 was used to obtain these two oil parameters in a range of temperatures. Results of these measurements are plotted in Figure 4. Surface tension was measured using the pendant drop method at ambient temperature, using an optical tensiometer (Attension Theta Optical Tensiometer). Surface tension at different temperatures was not possible to measure with the current configuration of the equipment. Results of this measurements are presented in the following Table 2. The tendency of this oil property is expected to vary with temperature similar to the density; and therefore with small differences between formulations.

Oil formulation	Ambient temperature [°C]	Surface tension [mN/m]	Surface tension difference [%]
SAE 5W30	26	28.36	-5.15
SAE 0W20	24	28.39	-5.05
SAE 0W16	23	29.87	-0.10
SAE 0W12	25	29.89	-0.03
SAE 0W8	23	29.90	0

Table 2: Surface tension of the oil formulations at ambient temperature

It can be seen from Figure 4 that kinematic viscosity does not vary significantly between oil formulations with SAE grade 0W; and these differences are smaller at higher temperatures, given the narrow viscosity ranges defined in the SAE J300 standard [29]. On the other hand, differences in viscosity for the same oil at different temperatures are more marked, specially for the SAE 5W30 oil. Regarding the surface tension, although there are small variations in the ambient temperature, due to the measurement conditions, differences between SAE 0W formulations are of 5% maximum, and of 5.15% for SAE 5W30, if SAE 0W8 is taken as reference, as shown in Table 2.

With these results, and taking into account that the aim was to evaluate levels of viscosity with significant differences, it was decided to select the 5W30 formulation for the tests, and vary the viscosity through the working temperature. The main characteristics of the oil are presented in the following Table 3, along with the additives concentration.

2.3. Test methodology

Two parameters of the engine working conditions were selected for the parametric tests, as they are expected to contribute to the formation and

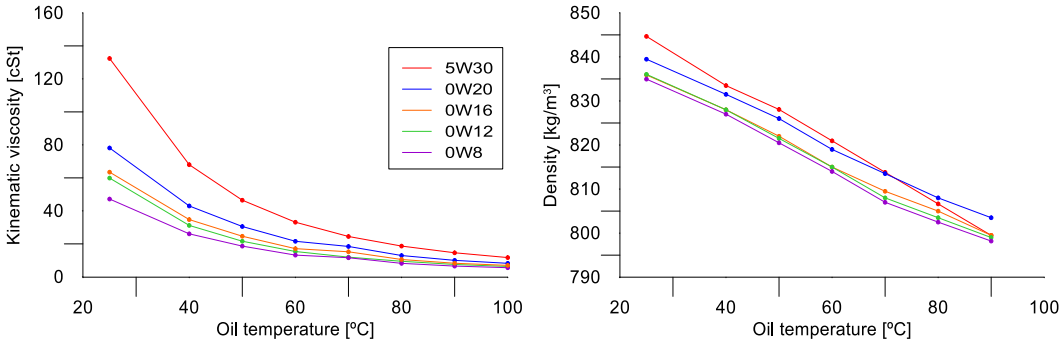

Figure 4: Kinematic viscosity and density of the oil formulations for different working temperatures

Parameter	Value	Parameter	Value
SAE grade	5W30	Calcium (Ca) [ppm]	1154
Kv* @ 40ºC [cSt]	68	Magnesium (Mg) [ppm]	9
Kv* @ 100ºC [cSt]	11.7	Barium (Ba) [ppm]	4
HTHS** @ 150ºC [cP]	3.5	Phosphorus (P) [ppm]	416
SAPS*** level	Low	Zinc (Zn) [ppm]	443
API base oil group	G-III + G-IV	Boron (B) [ppm]	1
		Molybdenum (Mo) [ppm]	0

Table 3: Main characteristics of the oil formulation. *Kinematic viscosity. **Hight Temperature High Shear viscosity. ***Sulphated Ash, Phosphorus and Sulphur

release of oil droplets to the combustion chamber of GDI engines. These are the engine speed, varied from 500 to 3000 rpm in intervals of 500, and the oil viscosity through its working temperature, tested at 40, 60 and 80ºC. Each test point consisted of six repetitions.

The procedure followed to develop one test repetition consisted first, in preparing a square of absorbing paper of 110x110mm with its corresponding reference name written in the lower right corner. This paper was weighed and photographed as reference for further image processing. Then, the paper was located in the sandwich-like support and held to the test rig structure as shown in Figure 3 a). Before every test, oil in the piston head and the cylinder liner wall was cleaned off. The rig was then operated at a constant engine speed, until reaching the desired oil temperature, followed by setting the engine speed for the test, and leaving 30 seconds for it to stabilize. Next, the cover plate of the paper support was removed and the test was executed

for 30 seconds. After finishing the test, the cover plate was put back and the engine speed set to zero. The paper support was removed from the rig and the paper weighed and imaged.

2.4. Oil mass calculation

A simple procedure was followed to calculate the mass of the oil droplets scattered to the combustion chamber. It consisted of weighing the absorbing paper before and after the test, in such a way that their difference gave the oil mass. From the repetitions of each test point, statistical parameters were calculated, mean and standard deviation of the oil mass measurements.

2.5. Oil droplet identification through image processing

Another way of measuring and identifying the oil droplets scattered to the combustion chamber was done through the processing of photographs taken to the absorbing paper and the oil trapped in it. Although this method didn't allow a quantitative analysis of the oil droplets released to the combustion chamber, it did help to identify potentially critical regions to the appearance of oil, and its correlation with the engine speed and oil viscosity. Furthermore, the grey level of spots identified as oil, was correlated with the oil mass weighed from the absorbing paper.

The methodology followed for this part of the study consisted of taking photographs of the absorbing paper with a reflex camera, before (White paper) and after (Oil paper) running the corresponding test. A set of raw images of the absorbing paper after running the test are presented in the Appendix A in Figure A.12, they correspond to 2000 rpm and 80°C of oil temperature. After finishing all the tests, the group of images was processed in mathematical software, Matlab. Each image was separated into its three color channels, (1: red, 2: green, 3: blue), and one of them was selected for the next steps. Selection of the color channel was done trying to obtain the most information from the image, and it was finally set for each engine speed, independent of the oil temperature. Figure 5 shows an example of the color channel separation corresponding to one test executed at 2000 rpm and 80°C of oil temperature. As shown in Figure 5 , for engine speeds of 2000 rpm, it seemed reasonable to select the red channel, where the oil spots are brighter.

With the channel selected for both the White paper and Oil paper, the reference name written in the lower right corner was replaced with a square of color equal to the mean RGB (Red, Green, Blue) value of the White paper.

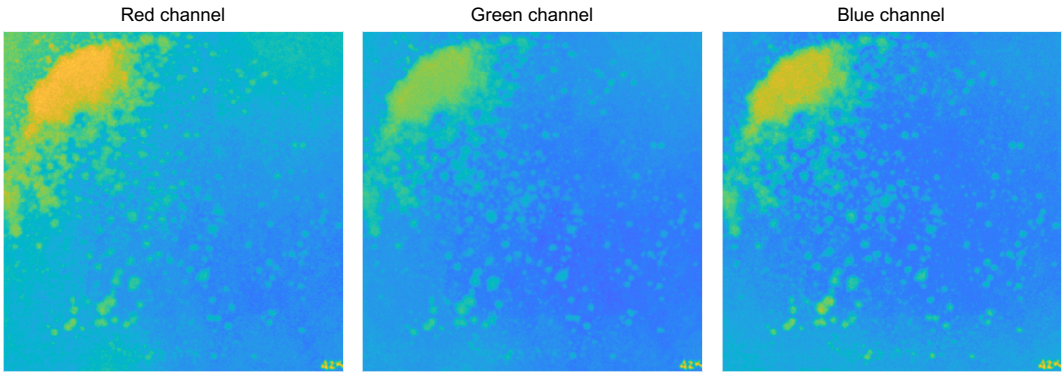

Figure 5: Separation of images in their three color channels. Example for 2000 rpm and 80°C of oil temperature

Then, images of Oil paper and White paper were subtracted to obtain the signal corresponding to the oil spots, as shown in Figure 6.

The next step consisted of defining a color threshold to separate the real oil spots from image noise. This threshold value was taken as a percentage of the maximum RGB value of the image obtained in the previous step (Figure 6) for each test repetition. Oil spots were then found as the pixels with RGB value higher than the predefined threshold. This step gave linear indices (coordinates) of the pixels' location. This step can be seen in the following Figure 7, where the original image and the spots identified as oil have been plotted in gray scale.

Finally, two statistical parameters were calculated, the probability distribution of the oil and the intensity of this distribution. The first one represents the probability of appearance of oil spots in a scale of 0 to 1, where 1 represents a probability of 100% and was calculated with the following expression (1).

$$Oil\ probability = \frac{\sum_{i=1}^{n} Binary\ matrix}{n} \tag{1}$$

The *Binary matrix* was obtained replacing the RGB values of the pixels identified as oil spots with ones and the rest of the matrix with zeros. n is the number of test repetitions. The second parameter, calculated with the expression (2), gives and indicative of the color intensity of the oil spots, and therefore of the quantity of oil in that specific region.

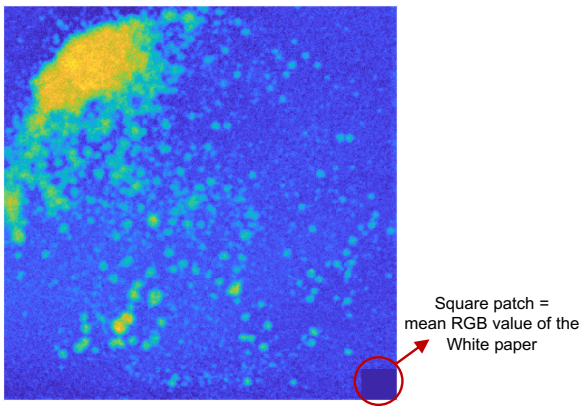

Figure 6: Oil spots image after subtraction of the White paper and Oil paper. Test ran at 2000 rpm and 80°C of oil temperature

$$Oil\ intensity = \frac{\sum_{i=1}^{n} I_{oil}}{n} \tag{2}$$

In this expression, I_{oil} corresponds to the color intensity of the pixels identified as oil, that is, with RGB values higher than the threshold.

3. Results and discussion

3.1. Oil mass scattered to the combustion chamber

Different hypothesis have been developed regarding the mechanism behind the scattering of oil droplets to the combustion chamber. The piston rings for instance, could scrap the oil from the cylinder wall during the reciprocating motion of the piston [3]. The effect of the fuel sprayed to the cylinder liner has also been suggested as a way of stripping the oil from the wall [30]. Welling et al [31] developed tests on a third hypothesis, where it was found that oil components with lower ignition delay times were carried to the combustion chamber by the blow-down gases, and provoked pre-ignition in the following engine cycle. In this study, the first mechanism of oil droplets release was studied as a result of the oil viscosity and engine speed.

As it was explained in section 2.4, oil released to the combustion chamber was measured as the quantity of mass trapped in the absorbing paper. Given that each test point comprised six repetitions, mean and standard deviation of the measurements were calculated. These results are shown in Figure 8

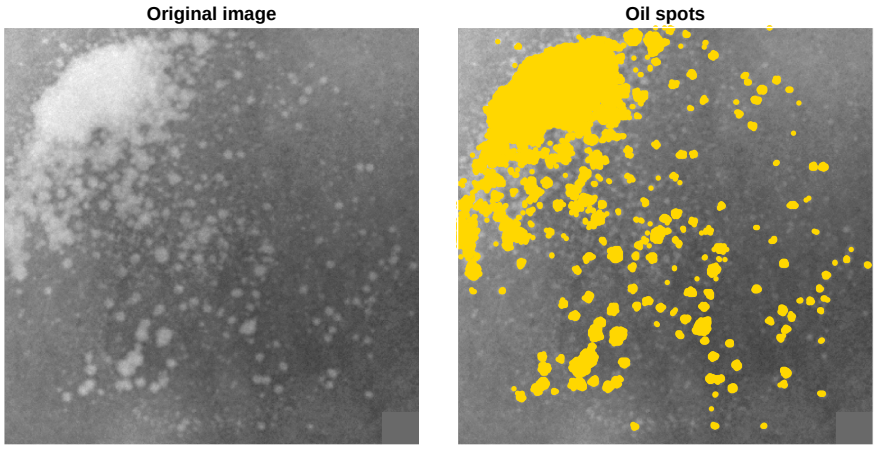

Figure 7: Real oil spots identification

for six engine speed levels and three oil temperatures. In Figure 8 a), results are presented as total oil mass for the 30 seconds period, while in Figure 8 b), the results were standardized for one engine cycle (720°). Tests at 1000 rpm were not possible to execute due to resonance of the test rig found at this engine speed; thus, tests were developed at 900 rpm. From Figure 8, it stands out the high deviation obtained at some engine speeds, especially at 1500 rpm and with the oil at 40°C. This deviation however, decreased with the oil temperature.

According to Figure 8, the correlation of oil droplets release to the combustion chamber with the engine speed is clearly marked, with a critical point at 2500 rpm and 80°C, where the oil mass scattered was greater than at 3000 rpm. The opposite trend was observed at 60°C; while at 40°C, this trend was affected by the high deviation in the measurements. Regarding the oil viscosity (oil working temperature), results show that this rheological characteristic does not have a determining effect on the oil droplets release. At 500 rpm by instance (Figure 8 b), tests run at 60°C have the lowest amount of oil; the same behavior is seen at higher engine speeds. On the other hand, results at 40 and 80°C are fairly similar, except for the test point at 2500 rpm.

Ito et al [18] came to a similar conclusion; they tested five oil formulations with different viscosity, and results of scattered oil quantity did not show a clear correlation with the oil viscosity. Regarding the engine speed, the oil mass released increased for some formulations when the speed was varied

from 900 to 1800 rpm. In the study developed by Kocsis et al [25], although the amount of oil droplets release was not measured, occurrence of LSPI events was correlated to the oil viscosity by means of analysis of variance (ANOVA). This analysis showed a connection between this property and lower LSPI rates when the low viscosity formulation had magnesium (Mg) instead of calcium (Ca), otherwise, no conclusive results were observed for the oil viscosity. Spicher et al [13] on the other hand, did find a decrease in the LSPI rate, of about 35%, using an oil formulation of higher viscosity.

In this study, the concentration of Mg in the oil formulation is low compared to the concentration of Ca, as it can be seen in Table 3. The concentration of these additives may not have an impact on the amount of droplets released to the combustion chamber, but on the reactivity of the droplet.

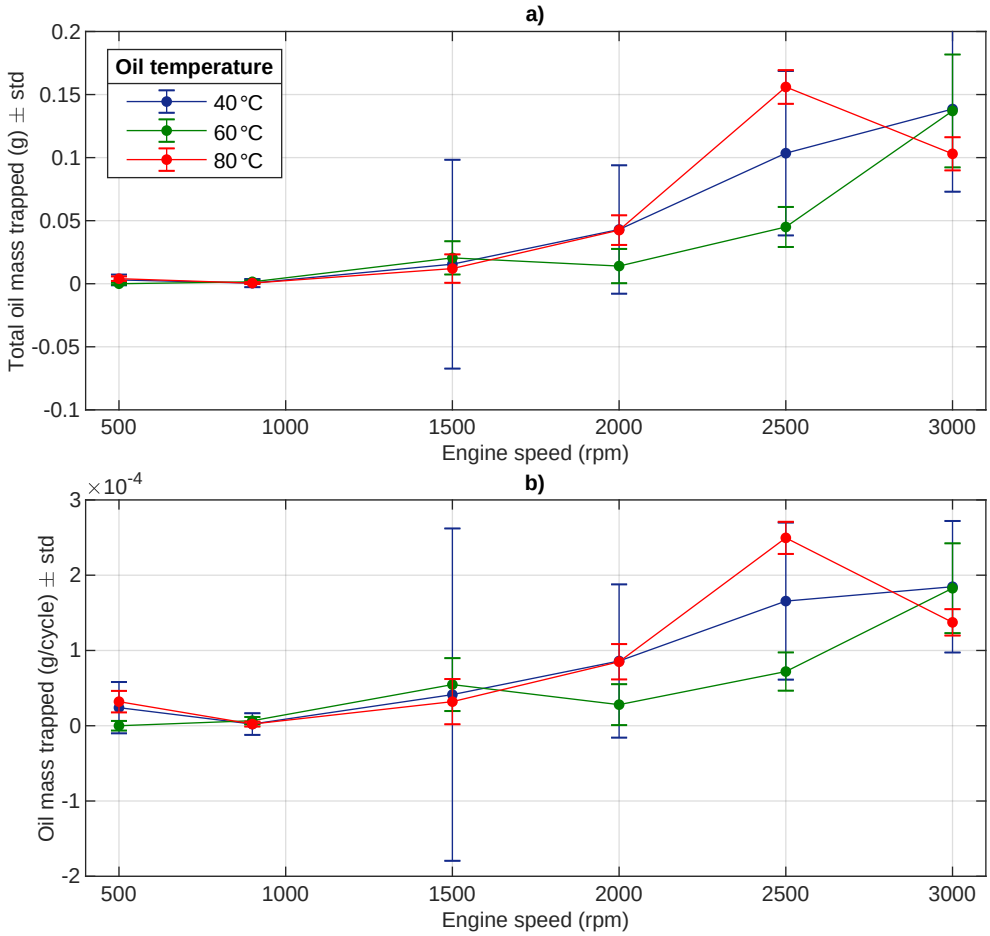

Figure 8: Mean oil mass and standard deviation of the measurement. a) is the total oil mass in a 30 seconds period. b) is the oil mass per cycle

3.2. Identification of oil droplets through image processing

Given the results of the previous section, where it was concluded that the oil viscosity does not have a determining effect on the oil droplets release, in this part of the study it was decided to gather the results by engine speed, independent of the oil temperature. Two parameters were calculated from the photographs taken to the absorbing paper and the oil trapped in it, the oil probability and its intensity. The first parameter presented in Figure 9, shows the probability of oil appearing at a specific location, that is, in a specific pixel of the image. Results are shown in a scale from 0 to 1, where 1 indicates that oil appeared in the absorbing paper in every test repetition for

the given engine speed. For the analysis of images, it is important to keep in mind that the absorbing paper was located upside down to collect the oil droplets, and it was turned for the photograph, as shown in Figure 3. In this way, the piston pin is horizontally aligned with the image, and the piston secondary motion occurs in the vertical axis.

Results shown in Figure 9 are highly related with those of the previous section 3.1, as expected. At low engine speed, 500 and 900 rpm, there is no oil scattering to the combustion chamber, except for a small region with about 50% probability of oil appearance, this region also appears at every engine speed. The source behind this oil region hasn't been determined, however, it could be related with the clearance between the cylinder liner and the piston, due to the absence of thermal expansion and the lack of appropriate sealing from the piston rings, which under ambient pressure conditions, only depends on the ring pre-tension. At 1500 rpm, regions with higher probability of oil appearance start to show, specifically at the thrust (upper part of the image) and anti-thrust (lower part of the image) locations, that is, in the axis of the piston secondary motion. As the engine speed increases, these two regions prone to oil appearance, seem to expand; at 2500 and 3000 rpm, the oil probability reaches 100% in both sides of the piston.

The appearance of oil spots at the sides of the piston, seems to indicate that the prevailing source of oil droplets is the piston crevice; however, there are regions with low oil probability at the center of the piston, which could also indicate oil accumulation in the piston crown that, due to the reciprocating motion of the piston, is scattered to the combustion chamber to a lower extent.

The second parameter obtained from the image processing is the oil intensity, shown in Figure 10. Given that this parameter represents the brightness of the pixel identified as oil, it allows to identify regions with greater amount of oil. On one hand, with the oil probability parameter, the most prone regions to the appearance of oil spots were identified; and on the other hand, with the oil intensity parameter it was possible to have an indicative of the amount of oil droplets released to the combustion chamber. If the images at 2500 and 3000 rpm are observed, it stands out the quantity of oil released in the axis of the piston secondary motion; specially at the upper part of the image, corresponding to the thrust side of the engine. This region of higher oil intensity starts to appear at 2000 rpm.

Furthermore, although the oil probability maps at 2500 and 3000 rpm are fairly similar, huge differences can be observed in the oil intensity maps,

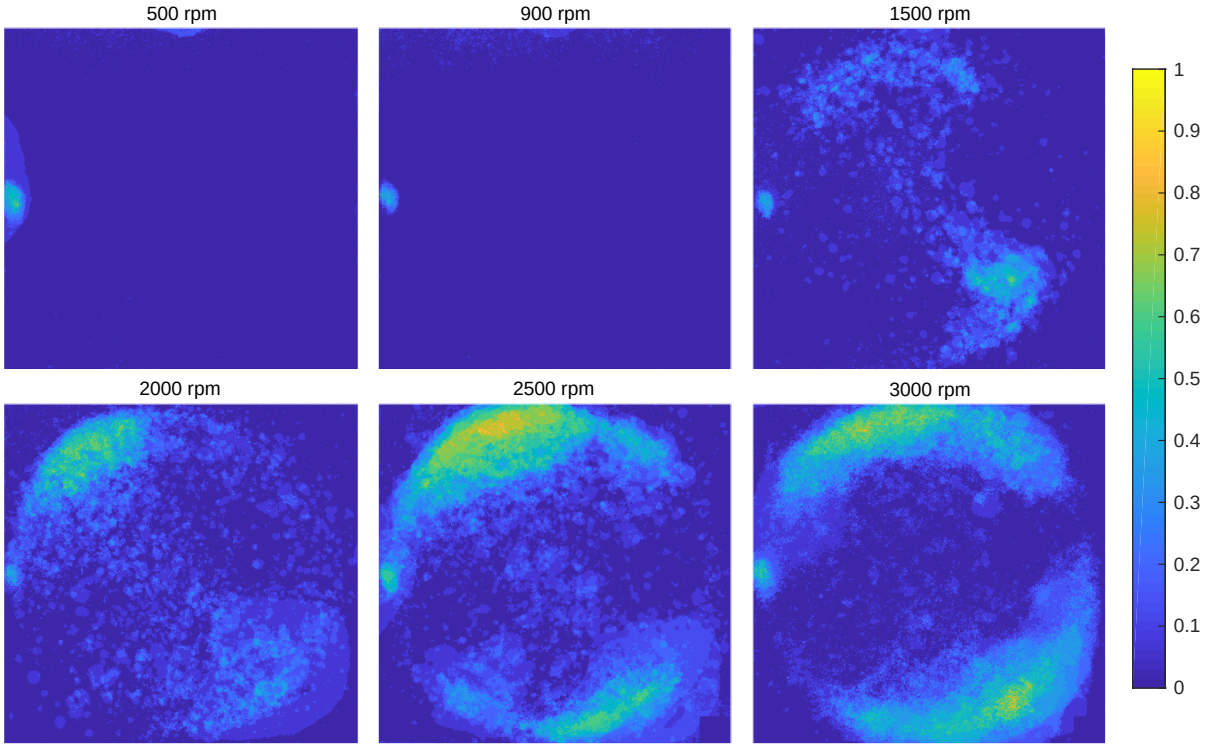

Figure 9: Oil probability for each engine speed independent of the oil temperature

where the oil mass trapped at 2500 rpm was significantly higher; thus demonstrating the importance of using the two parameters for the analysis. Results of oil intensity at 2500 rpm are also in line with those obtained in the previous section 3.1, where it was concluded that this regime is critical for the generation of oil droplets.

From Figure 10 it can also be observed that the small oil region that appears at every engine speed, presents a high oil intensity, that increases with the regime. An oil jet from the piston rings gap could be a source of oil; at the beginning of the tests, the piston rings were mounted in such a way that the angular distance between gaps would be of 120º, with the compression ring at 90º from the piston pin axis; therefore, given that the piston rings rotate around the circumference of the cylinder during engine operation [32], it seems improbable that one or all the piston rings would have aligned and maintained in the same position during tests.

Due to the configuration and working conditions of the test rig used in

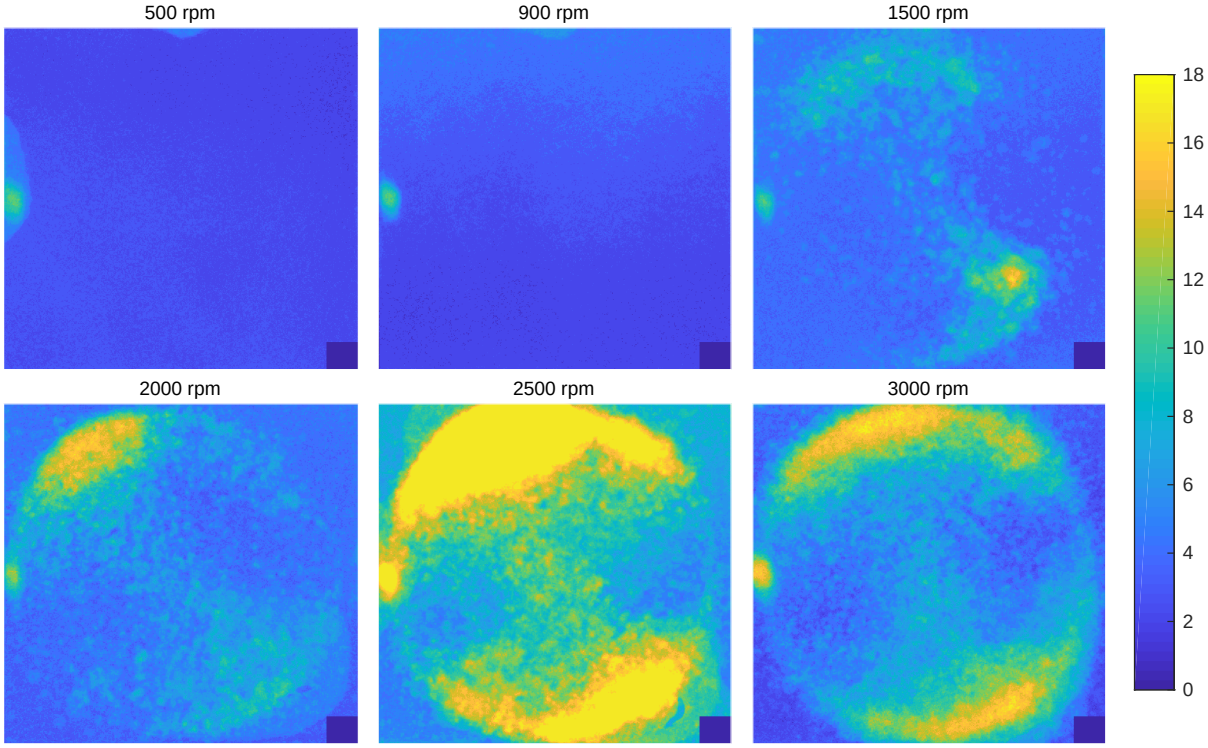

Figure 10: Oil intensity for each engine speed independent of the oil temperature

this study, results presented in this section can not all be directly correlated to an engine working under normal conditions. In cylinder pressure and gas motion, temperature of the piston-cylinder liner interface and thermal expansion, have an effect on the oil scattered to the combustion chamber. In an engine working under real conditions, pressure exerted on the back of piston rings creates an appropriate sealing with the liner and therefore, a smaller amount of oil would reach the combustion chamber. Regarding the critical zones for oil appearance, their location depends on the engine design, specially if the shape of the cylinder bore is not close to a perfect circle. On the other hand, the effect of the engine speed over the oil mass scattered, should not differ when running the engine under combustion conditions, as it depends on the inertial forces that contributes to the oil flow and accumulation of the oil in the upper part of the piston.

3.3. Comparison between methodologies

In this section a comparison between the two methodologies employed in this study, for the quantification and identification of oil droplets released to the combustion chamber, was developed. With the first methodology, it was possible to obtain a quantitative value of the oil mass released, by means of weighing the absorbing paper. Whereas for the second methodology, in order to obtain an estimation of the oil quantity that reaches the combustion chamber, the gray-level of the images was calculated, defined as the summation of intensities of the pixels identified as oil. Results of this analysis are shown in Figure 11, for the six engine speed levels (500 - 3000 rpm) and independent of the oil temperature, that is, each point comprises the results obtained for the three oil temperature levels.

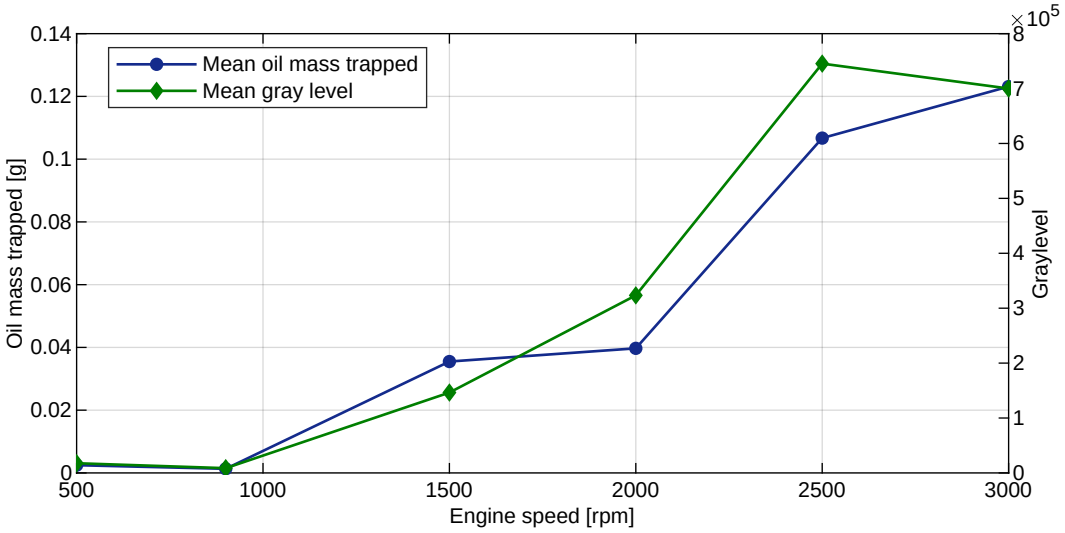

Figure 11: Comparison between the two methodologies employed for the quantification of oil mass released to the combustion chamber

From previous Figure 11, it can be observed that the grey-level of the processed images is in accordance with the oil mass measurements, and therefore offers a good estimations of the amount of oil released to the combustion chamber, and its correlation with the engine speed.

4. Conclusions

1. The small differences found on the physical properties of the oil formulations that share the same 0W SAE grade, kinematic viscosity and

density, lead to think that negligible differences could be found on the propensity to oil droplet release.

2. Oil droplets release was observed and measured for all the engine speed levels, even at 500 rpm, and specially with the increase of speed, with a critical point at 2500 rpm. This observation would lead to assume that LSPI events should occur at every cycle and increase its rate with speed, contrary to what has been found in literature. Therefore, these results show that other factors must be present for the oil droplet to ignite, such as the formation of a reactive mixture in terms of oil, air or even fuel, as well as adequate temperature and pressure conditions.
3. A good correlation was found between the two methodologies employed in this study for the measurement of oil mass released to the combustion chamber.
4. Taking into account that the working conditions of the test rig employed in this study do not fully represent that of normal engine operation, it was possible to identify critical regions of the combustion chamber prone to the appearance of oil droplets. These regions appeared transverse to the piston pin, in the axis of the piston secondary motion. Furthermore, the shape of these oil regions seems to indicate that the prevailing source of oil is the piston crevice. Nevertheless, oil also accumulates in the piston crown and is released to combustion chamber to a lower extent.
5. To fully understand the oil droplet release mechanism and its effect on the appearance of LSPI events, further studies are needed on the size of the droplets and the chemistry behind them.

Acknowledgments

Author Sophia Bastidas would like to thank the support of the program Ayudas de Investigación y Desarrollo (PAID-01-17) of the Universitat Politècnica de València.

Appendix A.

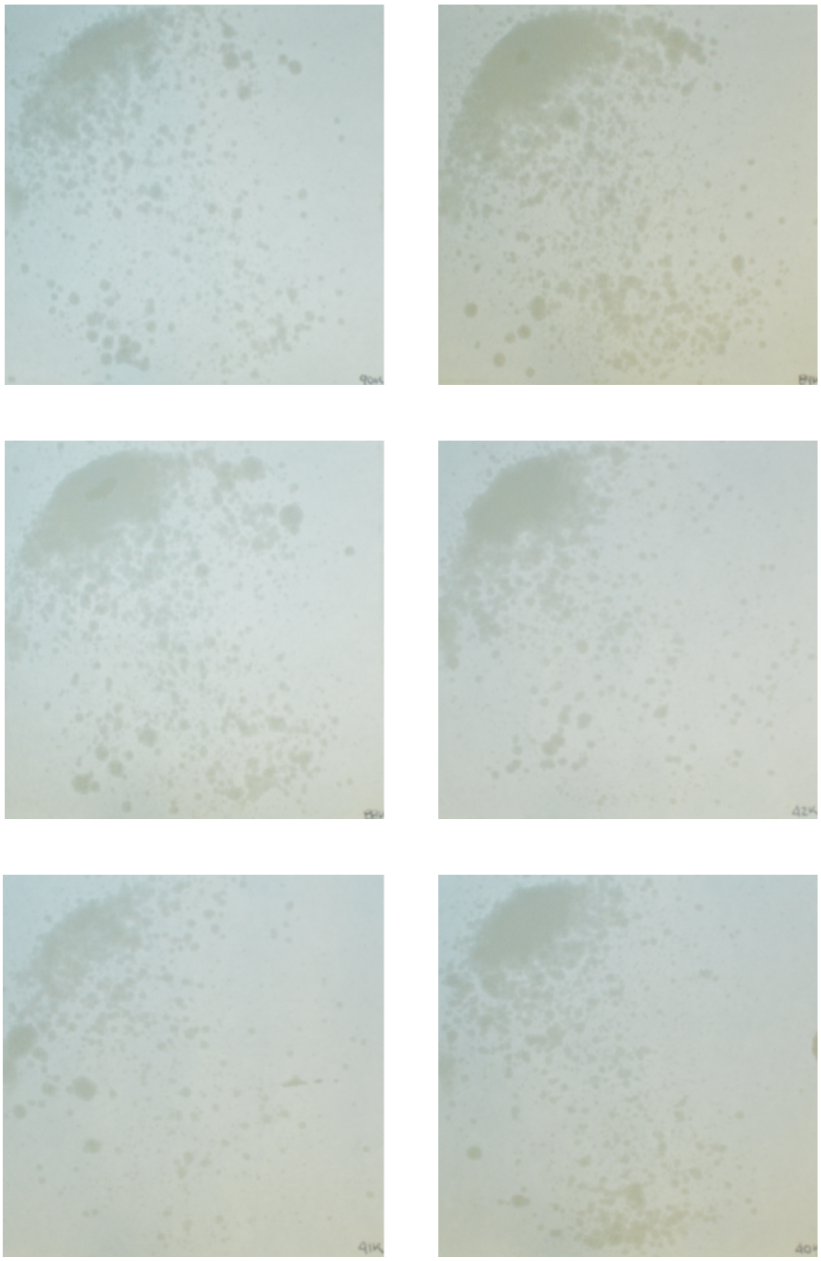

Figure A.12: Raw images of the absorbing paper with oil droplets scattered at 2000 rpm and 80º of oil temperature, and for the six repetitions

References

[1] E. M. Chapman, V. S. Costanzo, A literature review of abnormal ignition by fuel and lubricant derivatives, in: JSAE/SAE 2015 International Powertrains, Fuels and Lubricants Meeting, SAE International, 2015. doi:10.4271/2015-01-1869.

[2] G. S. Jatana, D. A. Splitter, B. Kaul, J. P. Szybist, Fuel property effects on low-speed pre-ignition, Fuel 230 (2018) 474–482. doi:10.1016/j.fuel.2018.05.060.

[3] C. Dahnz, K.-M. Han, U. Spicher, M. Magar, R. Schiessl, U. Maas, Investigations on pre-ignition in highly supercharged SI engines, in: SAE 2010 World Congress and Exhibition, SAE International, 2010. doi:10.4271/2010-01-0355.

[4] A. Zahdeh, P. Rothenberger, W. Nguyen, M. Anbarasu, S. Schmuck-Soldan, J. Schaefer, at al, Fundamental approach to investigate pre-ignition in boosted SI engines, in: SAE 2011 World Congress and Exhibition, SAE International, 2011. doi:10.4271/2011-01-0340.

[5] E. J. Passow, P. Sethi, M. Maschewske, J. Bieneman, K. Karrip, P. Truckel, An introduction to how low speed pre ignition affects engine components, in: WCX 17: SAE World Congress Experience, SAE International, 2017. doi:10.4271/2017-01-1042.

[6] A. Isenstadt, J. German, M. Dorobantu, D. Boggs, T. Watson, Downsized, boosted gasoline engines, Tech. rep., The International Council on Clean Transportation (2016).
URL https://theicct.org/publications/downsized-boosted-gasoline-engines

[7] B. Hu, S. Akehurst, C. Brace, Novel approaches to improve the gas exchange process of downsized turbocharged spark-ignition engines: A review, International Journal of Engine Research 17 (6) (2016) 595–618. doi:10.1177/1468087415599866.

[8] J.-M. Zaccardi, D. Escudié, Overview of the main mechanisms triggering low-speed pre-ignition in spark-ignition engines, International Journal of Engine Research 16 (2) (2015) 152–165. doi:10.1177/1468087414530965.

[9] I. Elliott, M. Sztenderowicz, K. Sinha, Y. Takeuchi, N. Ushioda, Understanding low speed pre-ignition phenomena across turbo-charged GDI engines and impact on future engine oil design, in: JSAE/SAE 2015 International Powertrains, Fuels and Lubricants Meeting, SAE International, 2015. doi:10.4271/2015-01-2028.

[10] M. Amann, T. Alger, D. Mehta, The effect of EGR on low-speed pre-ignition in boosted SI engines, in: SAE 2011 World Congress and Exhibition, SAE International, 2011. doi:10.4271/2011-01-0339.

[11] M. Amann, T. Alger, B. Westmoreland, A. Rothmaier, The effects of piston crevices and injection strategy on low-speed pre-ignition in boosted SI engines, in: SAE 2012 World Congress and Exhibition, SAE International, 2012. doi:10.4271/2012-01-1148.

[12] T. Kuboyama, Y. Moriyoshi, K. Morikawa, Visualization and analysis of LSPI mechanism caused by oil droplet, particle and deposit in highly boosted SI combustion in low speed range, in: SAE 2015 World Congress and Exhibition, SAE International, 2015. doi:10.4271/2015-01-0761.

[13] U. Spicher, M. Gohl, M. Magar, J. Hadler, The role of engine oil in Low-speed Pre-ignition, MTZ worldwide 77 (1) (2016) 60–63. doi:10.1007/s38313-015-0079-6.

[14] V. B. Kalaskar, A. Swarts, T. Alger, Impact of engine age and engine hardware on low-speed pre-ignition, in: International Powertrains, Fuels and Lubricants Meeting, SAE International, 2018. doi:10.4271/2018-01-1663.

[15] O. Welling, N. Collings, J. Williams, J. Moss, Impact of lubricant composition on Low-speed Pre-Ignition, in: SAE 2014 World Congress and Exhibition, SAE International, 2014. doi:10.4271/2014-01-1213.

[16] M. Kassai, K. Torii, T. Shiraishi, T. Noda, T. K. Goh, K. Wilbrand, S. Wakefield, A. Healy, D. Doyle, R. Cracknell, M. Shibuya, Research on the effect of lubricant oil and fuel properties on lspi occurrence in boosted s. i. engines, in: SAE 2016 International Powertrains, Fuels and Lubricants Meeting, SAE International, 2016. doi:10.4271/2016-01-2292.

[17] Y. Huang, Y. Li, W. Zhang, F. Meng, Z. Guo, 3D simulation study on the influence of lubricant oil droplets on pre-ignition in turbocharged DISI engines, Proceedings of the Institution of Mechanical Engineers, Part D: Journal of Automobile Engineering 232 (12) (2018) 1677–1693. doi:10.1177/0954407017734695.

[18] T. Ito, Y. Abe, J. Tanaka, Lubricating oil droplets in cylinder on abnormal combustion in supercharged SI engine, in: SAE/JSAE Small Engine Technology Conference, SAE International, 2018. doi:10.4271/2018-32-0008.

[19] M. Amann, T. Alger, Lubricant reactivity effects on gasoline spark ignition engine knock, in: SAE 2012 World Congress and Exhibition, SAE International, 2012. doi:10.4271/2012-01-1140.

[20] K. Takeuchi, K. Fujimoto, S. Hirano, M. Yamashita, Investigation of engine oil effect on abnormal combustion in turbocharged direct injection - spark ignition engines, in: SAE 2012 International Powertrains, Fuels and Lubricants Meeting, SAE International, 2012. doi:10.4271/2012-01-1615.

[21] T. Miyasaka, K. Miura, N. Hayakawa, T. Ishino, A. Iijima, H. Shoji, K. Tamura, T. Utaka, H. Kamano, A study on the effect of a calcium-based engine oil additive on abnormal SI engine combustion, in: SAE/JSAE 2014 Small Engine Technology Conference and Exhibition, SAE International, 2014. doi:10.4271/2014-32-0092.

[22] K. A. Fletcher, L. Dingwell, K. Yang, W. Y. Lam, J. P. Styer, Engine oil additive impacts on low speed pre-ignition, in: SAE 2016 International Powertrains, Fuels and Lubricants Meeting, SAE International, 2016. doi:10.4271/2016-01-2277.

[23] A. Ritchie, D. Boese, A. W. Young, Controlling low-speed pre-ignition in modern automotive equipment part 3: Identification of key additive component types and other lubricant composition effects on low-speed pre-ignition, in: SAE 2016 World Congress and Exhibition, SAE International, 2016. doi:10.4271/2016-01-0717.

[24] M. Mayer, P. Hofmann, B. Geringer, J. Williams, J. Moss, P. Kapus, Influence of different oil properties on low-speed pre-ignition in turbocharged direct injection spark ignition engines, in: SAE 2016 World

Congress and Exhibition, SAE International, 2016. doi:10.4271/2016-01-0718.

[25] M. C. Kocsis, T. Briggs, G. Anderson, The impact of lubricant volatility, viscosity and detergent chemistry on low speed pre-ignition behavior, in: WCX^{TM} 17: SAE World Congress Experience, SAE International, 2017. doi:10.4271/2017-01-0685.

[26] API, Latest oil classifications, [Accessed: 17/10/2019].
URL https://www.api.org/products-and-services/engine-oil/eolcs-categories-and-classifications/latest-oil-classifications

[27] A. Stone, V. Villena-Denton, API SN Plus: fast tracking new engine oil specifications, Fuels and Lubes International 23 (4) (2017) 20–21.

[28] Insight, Why ILSAC GF-6?, [Accessed: 25/10/2019].
URL https://www.infineuminsight.com/resources/ilsac-gf-6/why-ilsac-gf-6/

[29] SAE International, SAE J300 Engine Oil Viscosity Classification, United States (2015).

[30] G. T. Kalghatgi, D. Bradley, Pre-ignition and super-knock in turbo-charged spark-ignition engines, International Journal of Engine Research 13 (4) (2012) 399–414. doi:10.1177/1468087411431890.

[31] O. Welling, J. Moss, J. Williams, N. Collings, Measuring the impact of engine oils and fuels on low-speed pre-ignition in downsized engines, in: SAE 2014 World Congress and Exhibition, SAE International, 2014. doi:10.4271/2014-01-1219.

[32] E. W. Schneider, D. H. Blossfeld, Method for measurement of piston ring rotation in an operating engine, in: International Congress and Exposition, SAE International, 1990. doi:10.4271/900224.